# MIMO Virtual Array Design for mmWave 4D-Imaging Radar Sensors

Nazila Karimian Sichani[†1], Mohammad Alaee-Kerahroodi[⋆], Ehsan Raei[⋆]
Bhavani Shankar M. R.[⋆], Esfandiar Mehrshahi[†], Seyyed Ali Ghorashi [§,†]

[†]*Department of Telecommunications, Faculty of Electrical Engineering, Shahid Beheshti University, Tehran 1983963113, Iran.*
[⋆]*Interdisciplinary Centre for Security, Reliability and Trust (SnT), University of Luxembourg, Luxembourg.*
[§]*Department of Computer Science and Digital Technologies, School of Architecture, Computing and Engineering, University of East London, E16 2RD, London, UK.*

***Abstract*—The recently developed 4D-Imaging mmWave MIMO radars have significant advantages over conventional radar sensors because they offer a large virtual array in both azimuth and elevation. However, the physical placement of transmit and receive antennas to achieve the desired virtual array, while considering cost and efficiency is not intuitive. In this paper, we propose an optimization framework for optimally placing the transmit and receive array physical elements. The proposed framework obtains a sequence of optimal placements based on the coordinate descent by defining a desired virtual array and number of transmit and receive antenna elements as the objective. The objective function is then monotonically minimized in each iteration of the proposed algorithm, converging to a solution that guarantees the desired number of transmit and receive antenna elements, while the obtained virtual array is as close to the desired virtual array as possible. The simulation results are validated by simulating the virtual array of multiple commercially available 4D-Imaging radar products.**

***Index Terms*—4D-Imaging Radar, MIMO radar, Virtual Array, mmWave antenna configuration, Automotive radars.**

## I. Introduction

4D-Imaging millimeter-Wave (mmWave) radars are next-generation radar systems that demonstrate new ways for Highly Automated Driving (HAD) and Advanced Driver Assistance Systems (ADAS) to improve automotive safety. The state-of-the-art automotive radars use Multiple-Input Multiple-Output (MIMO) radar technology [1] as an attractive alternative to the full antenna array. For 4D-Imaging radars, a large number of antenna elements, such as a planar array with $576$ elements, are required, resulting in a significant cost for a radar sensor if the antenna elements are built physically. Alternatively, the physical elements can be efficiently created virtually, if sparse configuration be used on one side of the transmit (Tx) or receive (Rx) chain.

Recently, several works on the antenna array design and placement for 4D-Imaging MIMO radars has been carried out [2]–[6]. A novel 2D planar antenna array design was introduced in [2] that enables the three dimensional object detection in 4D radar imaging application by creating a wide Field of View (FoV) in azimuth direction. In [3], imaging performance in a 3D-Imaging radar improved by using antenna array sparsity which is achieved by a two step synthesis procedure. The number of elements is reduced while improving angular resolution. Furthermore, by adjusting the antenna positions, the lowest possible side-lobe level is achieved. The Vayyar Walabot-60GHz radar [4], which has a dense planar virtual MIMO array with a half-wavelength antenna spacing by default, is used to confirm the model. In [5], a system has been proposed with $36$ Tx and $48$ Rx channels, resulting in $1728$ virtual channels, working in 79 GHz frequency. This antenna array is realized with $12 \times 6$ Monolithic Microwave Integrated Circuits (MMIC)s, providing a high resolution in both azimuth and range. In addition to the studies cited above, [7]–[11] consider various approaches for determining optimal antenna placement, and then use computational approaches to solve the obtained problems. In [12] in a similar work, considering the lack of the analytically solved inverse mapping from the virtual array to the real transmitter-receiver configuration, the authors proposed a genetic algorithm to search the optimal antenna placement based on the ambiguity function and the antenna beampattern. The majority of these studies have focused on the problem of beampattern matching design with a Uniform Linear Array (ULA) setup, and antenna selection is accomplished by selecting $N$ from $M$ antennas and iteratively determining the best antenna position vector via optimization techniques.

To the best of our knowledge, the problem of obtaining transmit and receive antenna positions for a desired virtual array elements configuration is not analytically solved yet. Pursuing this objective, in this paper, (a) we formulate the problem of designing a MIMO virtual array with two objective functions. The first one aims at minimizing the Mean-Squared-Error (MSE) between the designed virtual array and a given one, while antenna elements are assumed to be placed in a grid-point planar configuration. To design the virtual array with a specified number of Tx/Rx array elements, the second objective function strives to minimize the difference between the number of designed and desired array elements; (b) We propose an iterative method based on the Coordinate Descent (CD) algorithm for solving the formulated optimization problem employing scaling factors between the two objectives.

[1]This paper was developed while Nazila Karimian Sichani was visiting SPARC at SnT, University of Luxembourg.

Output of each iteration is used as an input for the next iteration; (c) The simulation results show the proposed method with a monotonically decreasing cost function which leads to the optimum binary Tx/Rx position matrices at the convergence.

The rest of this paper is organized as follows[1]. In Section II, the problem formulation and the related optimization is discussed. Then, we introduce the proposed method for designing antenna array configuration and obtaining the desired virtual array based on CD algorithm in Section III. Simulation and numerical results are discussed in Section IV. Finally, Section V provides conclusion to the paper.

## II. Problem Formulation

We consider the problem of designing the configuration of Tx and Rx array antenna elements, in order to achieve a desired MIMO virtual array. Let $\mathbf{P}_t \in \{0,1\}^{M_t \times N_t}$ and $\mathbf{P}_r \in \{0,1\}^{M_r \times N_r}$ be defined as the Tx and Rx array antenna elements positions, respectively. Here, we assume a Uniform Rectangular Array (URA), i. e., a 2D planar configuration, for Tx and Rx antenna elements with $M_t$ and $N_t$ ($M_r$ and $N_r$) as the dimensions of Tx (Rx) array elements position matrix, in the coordinate plane with equal grid spacing $d = \lambda/2$, where $t_{\tilde{i},\tilde{j}} \in \{0,1\}$ and $r_{\bar{i},\bar{j}} \in \{0,1\}$ denote the position of the $(\tilde{i},\tilde{j})$-th Tx and $(\bar{i},\bar{j})$-th Rx array element, respectively, and $\lambda$ is the wavelength of the transmitted signal. $t_{\tilde{i},\tilde{j}} = 1$ (or $r_{\bar{i},\bar{j}} = 1$) indicates that a Tx (or Rx) antenna element is placed on the $(\tilde{i},\tilde{j})$-th (or $(\bar{i},\bar{j})$-th) grid point location of the URA; otherwise $t_{\tilde{i},\tilde{j}} = 0$ (or $r_{\bar{i},\bar{j}} = 0$). The MIMO virtual array ($\mathbf{V}$) is constructed by convolving the locations of the real Tx and Rx as $\mathbf{V} = \mathbf{P}_t * \mathbf{P}_r$ [13]. Due to overlap between antennas in virtual array elements, thus $\mathbf{V} \in \mathbb{Z}^{+^{(M_t+N_t-1)\times(M_r+N_r-1)}}$.

In order to design the MIMO virtual array and achieving the required number of Tx/Rx array elements simultaneously, we define the following bi-objective optimization problem:

$$\begin{cases} \min\limits_{\mathbf{P_t},\mathbf{P_r},\alpha} & \eta f_1 + (1-\eta) f_2 \\ s.t. & \begin{array}{ll} \mathbf{P}_t(\tilde{i},\tilde{j}) = \{0,1\}, & \forall \tilde{i} \in \{1,...,M_t\}, \\ \tilde{j} \in \{1,...,N_t\} & \\ \mathbf{P}_r(\bar{i},\bar{j}) = \{0,1\}, & \forall \bar{i} \in \{1,...,M_r\}, \\ \bar{j} \in \{1,...,N_r\} & \end{array} \end{cases} \tag{1}$$

where

$$f_1 = ||\mathbf{V}_d - \alpha \mathbf{P}_t * \mathbf{P}_r||_F, \tag{2}$$

$$f_2 = \big|||\mathbf{P}_t||_0 - L_T\big| + \big|||\mathbf{P}_r||_0 - L_R\big|. \tag{3}$$

$\mathbf{V}_d \in \mathbb{Z}^{+^{(M_t+N_t-1)\times(M_r+N_r-1)}}$ is the desired MIMO virtual array and $\alpha$ is a scaling parameter that should be optimized. The objective function $f_1$ is defined as a Frobenius norm of the distance between a desired virtual array and the designed one. The objective $f_2$ is the distance between the number of designed and desired array elements. Both objective functions are normalized. $\eta \in [0,1]$ is a scaling factor and $L_T$ and $L_R$ are the required number of Tx and Rx elements, respectively. With this form, we can achieve a desired virtual array with the specified number of Tx and Rx antenna array elements. The current optimization problem is multi-objective and non-convex. To tackle this challenge, we employ the CD framework to obtain a local solution for it.

[1]Notation: $\mathbb{R}^N$ denote the N-dimensional real vector space. We use boldface upper case $\mathbf{X}$ for matrices and boldface lower case $\mathbf{x}$ for vectors. $vec(.)$ is the vectorization operator. $||.||_F$ and $||.||_0$ are the Frobenius and zero norm of the matrix $\mathbf{X}$, respectively. Also, the $(m,n)$-th element of a matrix is denoted by $\mathbf{X}_{m,n}$. Also, $*$ denotes the convolutional operator. The transpose operator is denoted by $(.)^T$. $|x|$ denotes modulus of the complex number $x$ and $|\mathbf{x}|$ is a vector of element wise absolute values of $\mathbf{x}$, i.e., $|\mathbf{x}| = [|x_1|, |x_2|, \ldots, |x_L|]^T$.

## III. Proposed method

The optimization problem in (1), will be solved out over two different stages: 1) w.r.t. $\alpha$ for fixed $\mathbf{P}_t$ and $\mathbf{P}_r$, which has a closed-form solution for the related quadratic convex optimization, with a minimizer below:

$$\alpha = \frac{vec(\mathbf{V}_d)^T vec(\mathbf{P}_t * \mathbf{P}_r)}{||vec(\mathbf{P}_t * \mathbf{P}_r)||^2} \tag{4}$$

and 2) w.r.t. $\mathbf{P}_t$ and $\mathbf{P}_r$ for a fixed $\alpha$: $\mathbf{P}_t$ and $\mathbf{P}_r$ are binary matrices, so the problem with respect to these matrices is a discrete binary optimization problem. First, let us assume $\eta = 1$. To solve the problem, a Coordinate Descent (CD) approach is proposed, in which the multivariable problem is solved by changing the main problem into a sequence of single variable problems [6], [14]. Here, single variables are the positions of Tx and the Rx array elements. In each single variable optimization problem, for any entry of $\mathbf{P}_t$ and $\mathbf{P}_r$ ($t_{\tilde{i},\tilde{j}}$ and $r_{\bar{i},\bar{j}} \in \{0,1\}$), the minimizer to the problem will be kept in each iteration, while all the other elements are considered to be fixed. Then, the matrices $\mathbf{P}_t^i$ and $\mathbf{P}_r^i$ will be updated, subsequently. Here, $\mathbf{P}_t^i$ (or $\mathbf{P}_r^i$) is the updated Tx (or Rx) antenna array position matrix in the $i$-th iteration of the algorithm. This process will continue iteratively until the difference between two consecutive normalized objective functions is less than a pre-defined threshold.

Secondly, the above mentioned procedure will be repeated over a sequence of different values of scaling parameter $\eta \in [0,1]$. In the first step, where $\eta = 1$, a desired virtual array will be designed without considering the limitation on the number of Tx and Rx elements. Then, the output of the algorithm for $\eta = 1$ is considered as an input to the second iterative algorithm for another value of $\eta$, e.g. $\eta = 0.8$. In this case, the second normalized objective function $f_2$ attempts to reduce the number of Tx/Rx elements, while $f_1$ maintains the desired virtual array. When $\eta \to 0$, the algorithm can achieve the predefined number of Tx/Rx elements such that they guarantee the desired virtual array. The proposed algorithm, **TALA**, is summarized in **Algorithm 1**.

Note that to efficiently implement the convolution in iterations of CD method, we use the distributive property of convolution, that is $x_1[.,.] * (x_2[.,.] + x_3[.,.]) = x_1[.,.] * x_2[.,.] + x_1[.,.] * x_3[.,.]$ and the Dirichlet function convolution property, $x[n,m] * \delta[n-k, m-l] = x[n-k, m-l]$. In CD procedure, we calculate the convolution for every single variable, say each entry $(\bar{i},\bar{j})$ of the Tx and Rx array antennas,

**Algorithm 1** TALA: MIMO Virtual Array Design Algorithm for mmWave 4D-Imaging Radar Sensors.

**Inputs**: Initialize random array elements positions ($\mathbf{P}_t^0$ and $\mathbf{P}_r^0$), $\alpha = 1$, predefined threshold value $\epsilon$, a series of $\eta$ values $\in [0, 1]$, the number of required Tx and Rx array elements $L_T$, and $L_R$, and input $\mathbf{V}_d$.
**Outputs**: $\mathbf{P}_t^\star$ and $\mathbf{P}_r^\star$ (Solutions of (1)).
$j \leftarrow 1$;
Compute $f_1^0$ and $f_2^0$ from (2) and (3);
Compute $s(0) = \eta(j) f_1^0 + (1 - \eta(j)) f_2^0$;
**while** $j \leq$ length$(\eta)$ **do**
    **for** $i = 0, 1, 2, \ldots$ **do**
    $i \leftarrow i + 1$
    Update $\alpha^i$ using (4);
    Update $\mathbf{P}_t^i$ and $\mathbf{P}_r^i$ using CD;
    Compute $s(i) = \eta(j) f_1^i + (1 - \eta(j)) f_2^i$
    Break for loop if $s(i-1) - s(i) < \epsilon$;
    **end for**
$\mathbf{P}_t^\star = \mathbf{P}_t^i$ and $\mathbf{P}_r^\star = \mathbf{P}_r^i$.
$j \leftarrow j + 1$
**end while**
**Outputs**: $\mathbf{P}_t^\star$ and $\mathbf{P}_r^\star$.

for the two possible solutions in the binary set $\{0, 1\}$. To include this binary element change, we define $\Delta_{\bar{i}\bar{j}}$ as a matrix of size $\mathbf{P}_r$ with only a nonzero element in $(\bar{i}, \bar{j})$-th position such that $\Delta_{\bar{i}\bar{j}}(\bar{i}, \bar{j}) = 1$. In this manner, we can write the new virtual array while updating $(\bar{i}, \bar{j})$-th entry, $\mathbf{V}_{\bar{i}\bar{j}}^q$ based on the previous updated virtual array, $\mathbf{V}_{\bar{i}\bar{j}}^{q-1}$ as:

$$\begin{aligned}\mathbf{V}_{\bar{i}\bar{j}}^q =& \mathbf{P}_t^{q-1} * (\mathbf{P}_r^{q-1} \pm \Delta_{\bar{i}\bar{j}}) = \mathbf{V}_{\bar{i}\bar{j}}^{q-1} \pm (\mathbf{P}_t^{q-1} * \Delta_{\bar{i}\bar{j}}) \\ =& \mathbf{V}_{\bar{i}\bar{j}}^{q-1} \pm \mathbf{Z}_{\bar{i}\bar{j}}\end{aligned} \tag{5}$$

where $\pm$ is for two scenarios of placing and not placing an antenna element in the position $(\bar{i}, \bar{j})$. The matrix $\mathbf{Z}_{\bar{i}\bar{j}} \in \mathbb{R}^{(M_t+N_t-1)\times(M_r+N_r-1)}$ is a matrix of zero elements with only a non zero sub-matrix $\mathbf{P}_r^{q-1}$ beginning from the $(\bar{i}, \bar{j})$-th positions of the matrix $\mathbf{Z}_{\bar{i}\bar{j}}$. In this way, we can reduce the complexity of the large matrices convolution with only a simple summation operator and enhance the run time of the algorithm, significantly. Here, the equations are written for the case where CD method is applied to update Rx array position matrix. For the Tx one, we can rewrite the equations, similarly.

## IV. Numerical Examples

In this section, we provide numerical examples in order to assess the performance of the proposed algorithm. To that end, we first consider a virtual array of some Commercial Off-The-Shelf (COTS) as the desired virtual array, and then set the number of Tx/Rx antennas equal to the ones already considered for the COTS. In this case, we anticipate mimicking the virtual array of the COTS, but not necessarily with identical Tx/Rx physical configurations. This gives chip designers additional insight on the placement of Tx/Rx antenna elements while still satisfying the same virtual array. Furthermore, given

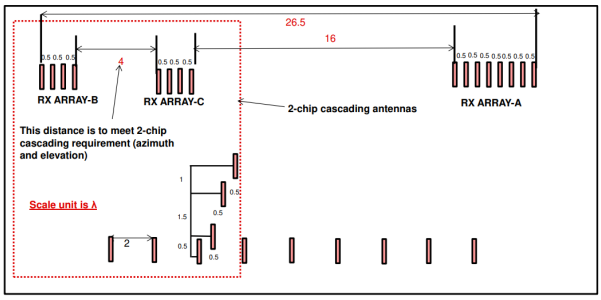


Fig. 1: Antenna Array Positions. Image taken from [15]

different initializations for $\mathbf{P}_t^0$ and $\mathbf{P}_r^0$ in **Algorithm 1**, a new configuration for Tx/Rx antenna elements can be obtained, expanding the design possibilities for chip designers in practical applications.

In addition, we can show how to construct an arbitrary virtual array, which may or may not be feasible given the number of physical Tx/Rx antenna elements. It would be possible to demonstrate that using the proposed framework, the design procedure can be close to the desired virtual array configuration while satisfying the number of Tx/Rx antenna elements.

**Example 1**: In the first example, we consider TI imaging radar (from Texas Instruments), with $L_T = 12$ Tx and $L_R = 16$ Rx channels. The Tx/Rx antenna array positions are based on AWR2243 cascade 4D-Imaging radar (see Fig. 1) [15]. In our problem, we consider the virtual array of this configuration as the desired one ($\mathbf{V_d}$), with $M_t = 64$ and $N_t = 12$, and also $M_r = 64$ and $N_r = 1$ separated grid points in a coordinate plane with a half-wavelength inter-grid interval, i.e. $d = \lambda/2$ that can be applied to place antennas. Using a decreasing scheme for $\eta$ values as described for **Algorithm 1**, we examine the convergence behaviour of the proposed method in Fig. 2a. We set $\epsilon = 10^{-5}$ in all of our simulations. It can be seen that, the normalized objective function of the optimization problem in (1) has a monotonically decreasing cost function value. This is due to the nature of CD method, which guarantees a decrement in the objective values. The desired and the designed MIMO virtual array are also depicted in Fig. 2b. The obtained locations of the Tx/Rx antenna elements on a grid-point 2D planar array, which lead to the designed virtual array, are shown in Fig. 2c, which corresponds to the antenna array positions in [15] and confirms the proposed algorithm.

**Example 2**: The used radar system platform, as a second case study, has been described in [2]. Here, a MIMO array with $L_T = 4$ and $L_R = 16$ has been used. We applied this setting to our proposed design method with $M_t = 16$, $N_t = 48$, $M_r = 16$, and $N_r = 32$. The objective function is depicted in Fig. 2d. Fig. 2e demonstrates the desired and designed related MIMO virtual array. The obtained Tx/Rx array configuration is also depicted in Fig. 2f that confirms the design described in [2].

**Example 3**: In this example, a 79 GHz high-resolution 4D-Imaging MIMO radar with 1728 virtual channels proposed

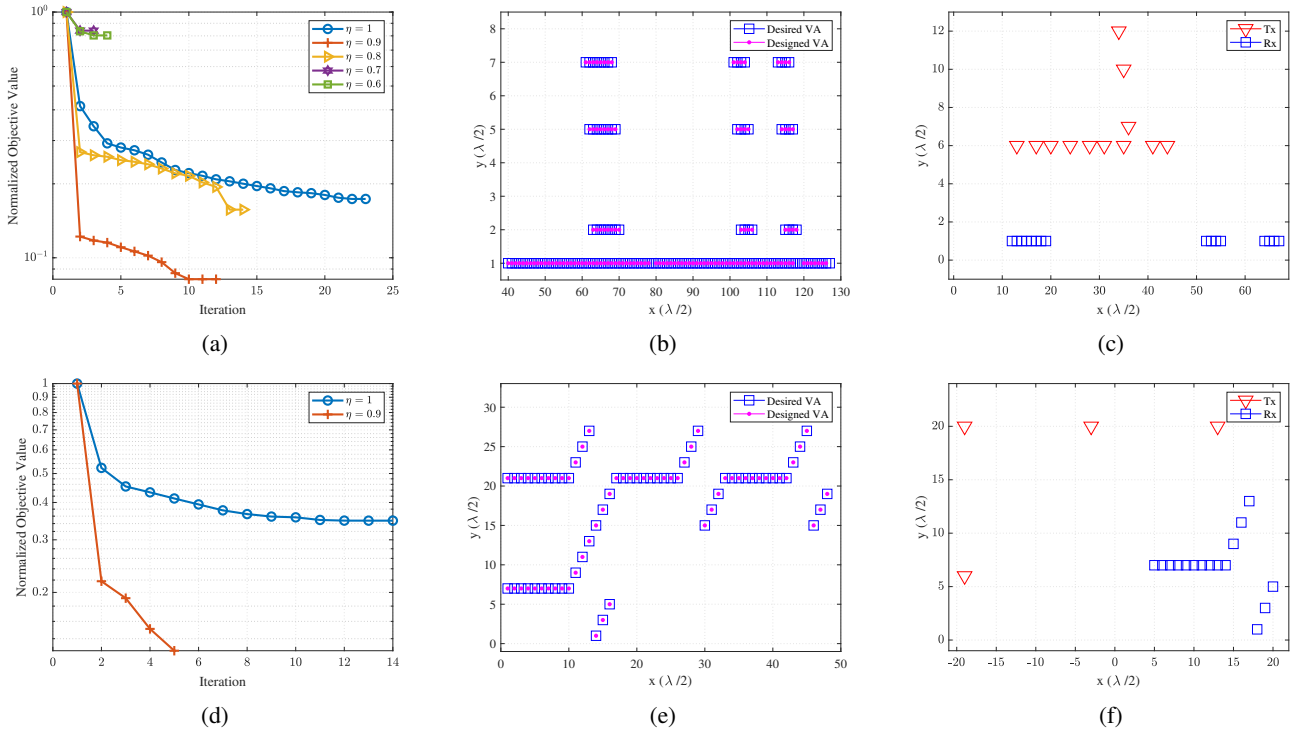


Fig. 2: Upper row (the desired virtual array from [15]): (a) Convergence curve of the proposed algorithm for different $\eta$ values. (b) Dense configuration of designed and desired virtual array (VA). (c) Obtained Tx/Rx antenna positions. Bottom row (the desired virtual array from [2]): (d)-(f) the same as the upper row.

TABLE I: The number of transmitter and receiver obtained in each step of the proposed algorithm for different values of $\eta$.

| **Scaling Factor** | **[15]** | | **[4]** | | **[2]** | | **[16]** | | **[3]** | | **[17]** | | **[18]** | |
|---|---|---|---|---|---|---|---|---|---|---|---|---|---|---|
| | $L_T$ | $L_R$ | $L_T$ | $L_R$ | $L_T$ | $L_R$ | $L_T$ | $L_R$ | $L_T$ | $L_R$ | $L_T$ | $L_R$ | $L_T$ | $L_R$ |
| $\eta = 1$ | 40 | 23 | 24 | 24 | 28 | 17 | 25 | 52 | 20 | 20 | 86 | 19 | 36 | 190 |
| $\eta = 0.9$ | 24 | 18 | - | - | 4 | 16 | 25 | 45 | - | - | 24 | 18 | 36 | 48 |
| $\eta = 0.8$ | 13 | 16 | - | - | - | - | 24 | 24 | - | - | 23 | 16 | - | - |
| $\eta = 0.6$ | 12 | 16 | - | - | - | - | - | - | - | - | - | - | - | - |

in [5] is considered as the other case study. The proposed radar system is composed of 12 transceiver MMICs, each one contains 3 Tx and 4 Rx channels. The antennas are placed in a 2 mm grid points in azimuth (a slightly larger than $\lambda/2$) and 2.5 mm in elevation. To enable transmit beamforming, each of the 6 transmit antennas is grouped as a $2 \times 3$ URA configuration. The convergence of the proposed algorithm is shown in Fig. 3a. Also, The dense representation of the virtual array of this configuration is shown in Fig. 3b, with $L_T = 36$ Tx and $L_R = 48$ Rx antenna elements, which is obtained by setting $M_t = 95$, $M_r = 20$, $N_t = 99$, $N_r = 25$. The resulting 2D array configuration is also depicted in Fig. 3c.

In Table 1, we compare the obtained virtual array of different case studies when their virtual array was used as the desired one. As shown in the table, the proposed algorithm is able to mimic the desired virtual array in all of the examples. The table also shows how many Tx/ Rx array elements each example obtained at various steps of the algorithm.

Finally in Fig. 4, we show that the algorithm is able to mimic an arbitrary virtual array, which is a circular array in this example. We consider our design with $L_T = 23$ and $L_R = 16$, and set $M_t = N_t = 23$ and $N_t = N_r = 5$.

## V. Conclusion

In this paper, the problem of designing a desired virtual array and the Tx/Rx antenna positions to approximate the virtual array with a particular number of array elements was studied. In order to tackle the problem, we proposed a sequence of iterative algorithms based on CD method. Numerical examples were provided demonstrating the excellent performance of the proposed method for obtaining arbitrary configurations of different virtual arrays.

## References


[1] I. Bekkerman and J. Tabrikian, "Target detection and localization using MIMO radars and sonars," *IEEE Transactions on Signal Processing*, vol. 54, no. 10, pp. 3873–3883, 2006.

[2] Martin Stolz, Maximilian Wolf, Frank Meinl, Martin Kunert, and Wolfgang Menzel, "A new antenna array and signal processing concept for an automotive 4D radar," in *2018 15th European Radar Conference (EuRAD)*, 2018, pp. 63–66.

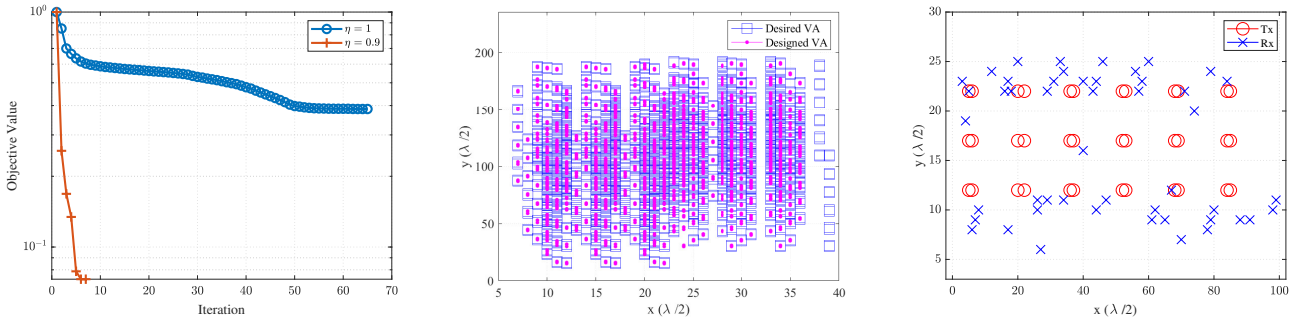


(a) (b) (c)

Fig. 3: (a) The convergence curve of the proposed algorithm, (b) Dense configuration of designed and desired virtual array (VA) [5] and (c) Obtained Tx/Rx antenna positions.

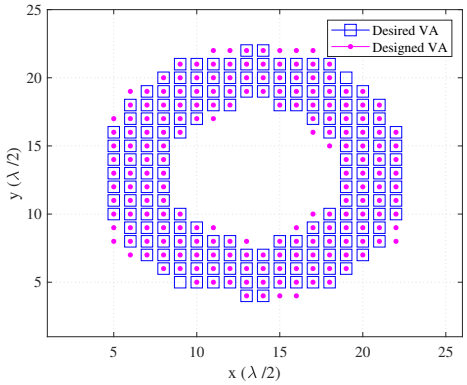


Fig. 4: Configuration of desired and designed virtual array.


[3] R. Z. Syeda, T. G. Savelyev, M. C. van Beurden, and A. B. Smolders, "Sparse MIMO array for improved 3D mm- Wave imaging radar," in *2020 17th European Radar Conference (EuRAD)*, 2021, pp. 342–345.

[4] "Vayyar 4d Imaging Radar on Chip," [Online]. Available:, https://vayyar.com/technology/#hardware.

[5] Dominik Schwarz, Christian Meyer, André Dürr, Ahmad Mushtaq, Wolfgang Winkler, and Christian Waldschmidt, "System performance of a scalable 79 GHz Imaging MIMO Radar with injection-locked lo feedthrough," *IEEE Journal of Microwaves*, vol. 1, no. 4, pp. 941–949, 2021.

[6] Ehsan Raei, Mohammad Alaee-Kerahroodi, and M.R. Bhavani Shankar, "Spatial- and range- ISLR trade-off in MIMO radar via waveform correlation optimization," *IEEE Transactions on Signal Processing*, vol. 69, pp. 3283–3298, 2021.

[7] Claudia Vasanelli, Rahul Batra, Adolfo Di Serio, Frank Boegelsack, and Christian Waldschmidt, "Assessment of a Millimeter-Wave antenna system for MIMO radar applications," *IEEE Antennas and Wireless Propagation Letters*, vol. 16, pp. 1261–1264, 2017.

[8] Zhang Haowei, Xie Junwei, Shi Junpeng, and Zhang Zhaojian, "Antenna selection in MIMO radar with collocated antennas," *Journal of Systems Engineering and Electronics*, vol. 30, no. 6, pp. 1119–1131, 2019.

[9] D. W. Bliss, K. W. Forsythe, and C. D. Richmond, "MIMO radar: Joint array and waveform optimization," in *2007 Conference Record of the Forty-First Asilomar Conference on Signals, Systems and Computers*, 2007, pp. 207–211.

[10] Ziyang Cheng, Yanxi Lu, Zishu He, Yufengli, Jun Li, and Xi Luo, "Joint optimization of covariance matrix and antenna position for mimo radar transmit beampattern matching design," in *2018 IEEE Radar Conference (RadarConf18)*, 2018, pp. 1073–1077.

[11] Minglong Deng, Ziyang Cheng, and Zishu He, "Co-design of waveform correlation matrix and antenna positions for MIMO radar transmit beampattern formation," *IEEE Sensors Journal*, vol. 20, no. 13, pp. 7326–7336, 2020.

[12] Claudia Vasanelli, Rahul Batra, and Christian Waldschmidt, "Optimization of a MIMO radar antenna system for automotive applications," in *2017 11th European Conference on Antennas and Propagation (EUCAP)*, 2017, pp. 1113–1117.

[13] Jian Li and Petre Stoica, *Adaptive Signal Design For MIMO Radars*, pp. 193–234, 2009.

[14] Ehsan Raei, Mohammad Alaee-Kerahroodi, Prabhu Babu, and M. R. Bhavani Shankar, "Design of MIMO radar waveforms based on lp-norm criteria," 2021.

[15] "Design guide: TIDEP -01012—Imaging radar using cascaded mmWave sensor reference design (REV. A)," Texas Instruments Inc., Dallas , June 2019, [Online]. Available: http://www.ti.com/lit/ug/tiduen5a/tiduen5a.pdf.

[16] Alexander Ganis, Enric Miralles Navarro, Bernhard Schoenlinner, Ulrich Prechtel, Askold Meusling, Christoph Heller, Thomas Spreng, Jan Mietzner, Christian Krimmer, Babette Haeberle, Steffen Lutz, Mirko Loghi, Angel Belenguer, Hector Esteban, and Volker Ziegler, "A portable 3-d imaging FMCW MIMO radar demonstrator with a $24 \times 24$ antenna array for medium-range applications," *IEEE Transactions on Geoscience and Remote Sensing*, vol. 56, no. 1, pp. 298–312, 2018.

[17] Dominik Schwarz, Nico Riese, Ines Dorsch, and Christian Waldschmidt, "System performance of a 79 ghz high-resolution 4d imaging mimo radar with 1728 virtual channels," *IEEE Journal of Microwaves*, vol. 2, no. 4, pp. 637–647, 2022.

[18] Kerry E. Dungan, Christian D. Austin, John W. Nehrbass, and Lee C. Potter, "Civilian vehicle radar data domes," in *Defense + Commercial Sensing*, 2010.